The SPARC_LAB Thomson Source

C. Vaccarezza (Resp. Naz.), M.P. Anania (Art. 23), M. Bellaveglia,P. Cardelli (Ass.), M. Cestelli Guidi (Art 23)
D. Di Giovenale (Art. 23), G. Di Pirro, A. Drago,M. Ferrario,F. Filippi (Ass.), A. Gallo, G. Gatti,
A. Ghigo, A. Giribono, (Ass), L. Lancia (Ass), A. Marcelli, A. Mostacci (Ass.), L. Palumbo (Ass.),
R. Pompili (Art.23), S. Romeo (Dott.), F. Villa (Art.23),
Participant Institutions: other INFN sections (BA, Ca, Fe, Le, LNS, Fi, Na, Pi, Mi, RM1, RM2), ENEA-Frascati

1 Introduction

The second commissioning shift of the SPARC_LAB Thomson source took place in June 2015 aiming to improve the $N_\gamma \approx 6\times 10^3$ photon flux measured in the very first attempt of Compton collisions in 2014. The SPARC_LAB Thomson source has been described elsewhere [8] and it consists in the SPARC photoinjector [2,3], that provides the $30 \div 150 MeV$ electron beam, coupled with the $300 TW$ FLAME laser system [2,6] in order to provide a X-ray Thomson source in the range of $20 \div 500 keV$. A $20m$ double dogleg carries the electron beam output from the photo injector down to the Thomson Interaction Point where the FLAME laser pulse is brought by a $20m$ in vacuum optical transfer line, see Fig. 1.

Since the first planned experiment with the Thomson radiation was the X-ray imaging of mammography phantoms with phase contrast technique [1,5,7], the source parameters of the electron and laser beams have been so far optimized to obtain the required flux of photons with moderate (20%) monochromaticity according to the simulation results described in [7] and are reported in Table1. For this commissioning phase anyway more relaxed parameters have been adopted and the obtained results are described in the following sections of this paper. Nevertheless is worth to notice the relevance of the SPARC_LAB Thomson source in terms of energy tunability that, for example, will provide the possibility to explore the ELI-NP Gamma Beam Source low energy range operation, since the electron beam energy is foreseen to range between 75 and 740 MeV. Certainly the opportunity to test the electron beam dynamics together with the electron and radiation diagnostic will play an important role in view of the ELI-NP machine future commissioning in Magurele under the INFN responsability. Moreover thanks to the FLAME laser system flexibility non linear regimes for the Compton scattering could be explored together with new experimental schemes that conjugate the Compton radiation production with the most advanced plasma based acceleration schemes for the electrons.

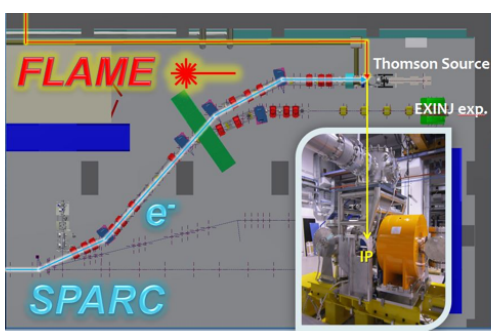

Figure 1: *SPARC_LAB Thomson source schematic layout.*

Table 1: Thomson Source Design Parameter list (2015 run)

Electron Beam	Energy	(MeV)	30
	Energy spread	%	< 0.1
	Charge	(pC)	$100 \div 800$
	Emittance	(mm mrad)	$1 \div 3$
Laser Beam	Wavelenghth	(nm)	800
	Pulse energy	(J)	$1 \div 5$
	Pulse length	(ps)	6
	Spot size	(μm)	10
	Repetition rate	(Hz)	10
X-ray Beam	Photon energy	(keV)	$20 \div 22$
	Photon number per shot		10^9
	Source rms radius	(ps)	10
	Bandwidth	%	$10 \div 20$

2 The Electron Beam

The electron beam is provided by the SPARC photoinjector [2, 3]; the working point for this second commissioning phase has been set up with $Q = 200pC$ beam and energy $E = 30MeV$. No RF attenuators are available in the RF systems of the three S-band TW sections that follow the gun, therefore an hybrid compression-deceleration scheme has been set with the following phases of the accelerating sections: $\Phi S1 = +32deg$, $\Phi S2 = -72deg$, $\Phi S3 = -134deg$ from crest, in order to minimize the effects of the power amplitude jitter from the feeding Klystrons, and obtain a final energy of $30MeV$ with an energy spread $\sigma_\delta \leqslant 0.1\%$. The envelope and beam emittance evolution through the photoinjector has been simulated with the ASTRA [4] and 50k particles; the results are shown in Fig. 2 and are in good agreement with the beam spot measurements (reported dots, crosses) taken at the screen locations along the linac. The longitudinal space of the electron beam at the exit of the photoinjector is measured by means of the S-band RF deflector coupled with a 14 dipole magnet and is reported in Fig. 3 as captured on the YAG screen located downstream the dipole.

From the photoinjector exit a double dogleg brings the electron beam to the interaction points of the Thomson experiment, its R_{56} parameter can be set in the range of 50 mm, closing the horizontal dispersion at the end of the last dogleg dipole. For the commissioning phase the dispersion is closed at the end of each dipole pair and the emittance evolution measurement is performed with the quadrupole scan technique in each straight section downstream the dipole pairs [8]. From the transverse emittance measurement performed at the linac exit the Twiss parameters are obtained to match the beam to the dogleg entrance for the transport to the Interaction Point. The final focusing is performed in the final straight section using a quadrupole magnet triplet and a solenoid, with a maximum field B=1.1T, close to the IP. At 30 MeV the minimum obtained spot size for the electron beam was around $\sigma_{rms} \approx 60 \div 80\mu m$ as reported in Fig. 4.

3 The Photon Beam

The laser pulse used to drive the Thomson back scattering process with the SPARC electron beam is provided by the FLAME laser system [6]. FLAME is a nominal $300TW$ laser system that uses 11 YAG pump lasers and 5 titanium-sapphire multi-pass amplifiers to produce linearly polarized pulses with a central wavelength $\lambda_0 = 0.800\mu m$ in a $60 \div 80nm$ bandwidth. The pulse duration ranges between $25fs \leqslant \tau_L \leqslant 10ps$,

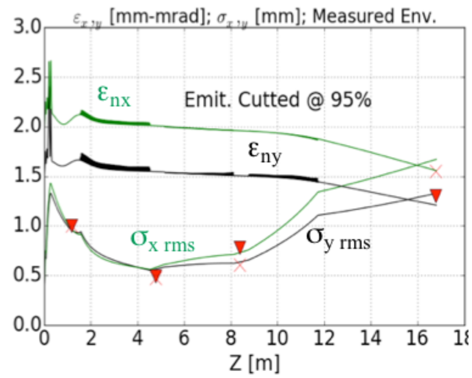

Figure 2: Electron beam emittance (hor, vert) and envelope (x,y) evolution from the photocathode to the linac exit calculated with the Astra code (Full 3D analysis). The dots and crosses represent the beam spot measurements (horizontal and vertical) taken in these configurations at screen locations along the linac.

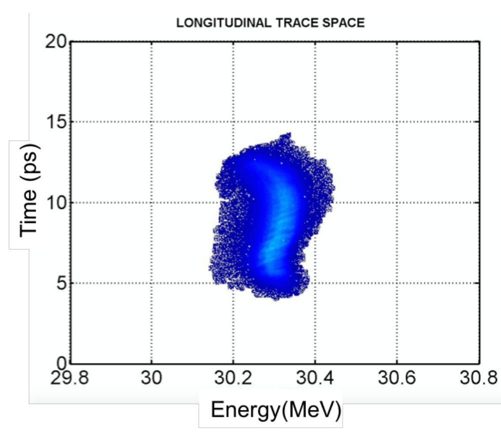

Figure 3: Longitudinal phase space image of the 30MeV electron beam coming out the SPARC photoinjector.

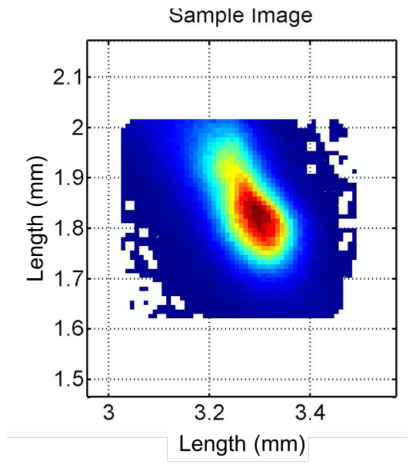

Figure 4: Electron beam spotsize at the IP, with $\sigma_{rms} \approx 60 \div 80\mu m$, vertical and horizontal respectively.

and the maximum energy is $E = 7J$ that corresponds to an energy on target $E_t \sim 5J$, at $10Hz$ repetition rate. The required focal spot has been obtained with the use of the adaptive optic placed inside the compressor.

4 Synchronization

The Thomson scattering experiment needs an extremely precise synchronization between electron bunch and laser pulse. The synchronous arrival of electrons and photons at the IP is obtained by locking the oscillators of the photo-cathode laser and interaction laser systems, and the phase of the RF accelerating fields to a common Reference Master Oscillator (RMO). The RMO is a low phase noise ($60fs_{RMS}$ integrated in the $10Hz \div 10MHz$ range) microwave oscillator tuned at the Linac main frequency 2856 MHz. The laser oscillators are locked through a PLL architecture to the 36th sub-harmonics of the RMO, while the output RF phase of the linac klystrons is downconverted to baseband by mixing with the RMO signal, and deviations are corrected both within the $4\mu s$ RF pulse duration (jitter feedback) and pulse-to-pulse (drift feedback).

5 X-ray beam Diagnostic

In the commissioning phase a detector that allows to measure the x-ray yield is required that must have a high sensitivity and a wide dynamic range to detect the potentially weak signal generated in the first non-optimised collisions. The detector we selected is a scintillator crystal coupled with a photomultiplier tube (PMT) located at $450cm$ downstream the Thomson IP. The crystal used is a CsI(Tl) of size (20x20x2) mm^3, coupled with a light-guide to a PMT (Hamamatsu, mod. R329-02). The signal is acquired using both an oscilloscope and a multichannel analyser (MCA-8000, Amptek, US) connected to a PC. Due to the high intensity and short duration of the pulse, it is not possible to distinguish the signal produced by the interaction of each single photon in a pulse, as in traditional spectroscopic application, but the signal is proportional to the entire energy released in the scintillator by each pulse. Therefore, an information on the energy distribution is required to evaluate the number of photon in each pulse.

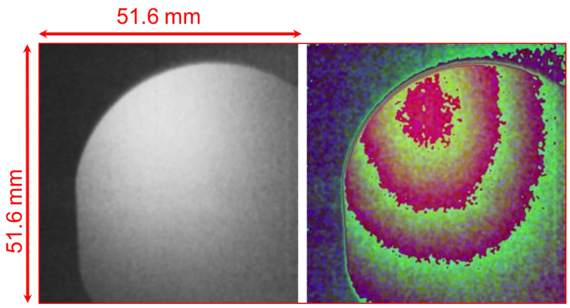

Figure 5: Thomson X-radiation image collected with Hamamatsu imager Flat Panel C9728DK-10, located at $300cm$ from the IP, with $1s$ exposure time and averaged over 100 images.

6 Commissioning results

For the selected WP with $200pC$ and 30 MeV electron beam at the Linac exit the measured normalized transverse emittance was $\varepsilon_{x-y} = 1.2 - 2.2 \pm 0.2\mu rad$, with an energy spread $\sigma_\delta = 0.1 \pm 0.03\%$, and a rms length $\sigma_z = 2.2 \div 0.2ps$. The minimum electron beam size reached was $\sigma_{x-y} \sim 60 - 80 \pm 10\mu m$. Due to background problems on the X-ray detectors, placed relatively close to the electron beam dumper, we should limit the IP electron spot size to $\sigma_{x-y} \sim 110 \pm 10\mu m$. In fact, due to a residual misalignment of the electron beam with the respect to the dumper vacuum pipe (enhanced by the strong focusing field of the solenoid B = 0.7 T), the background increased when the beam divergence was higher as consequence of a stronger focusing at IP. This misalignment was also detected by the imager recorded data that are shown in Fig.5 where the Thomson radiation image is clearly cut by the Perspex CF 40 window profile.

To measure the radiation energy two k-edge filters, Nb and Zr, were also used, resulting in a roughly estimated value of 13 keV, confirming the cut of the most energetic part of the produced radiation due to the tilted electron trajectory. In fact, with our commissioning setup the expected number of photons in the 20% bandwidth is:

$$N_\gamma = 4.8 \times 10^8 \frac{U_L\,[J]\,Q\,[pC]\,\delta_\phi}{h\nu\,[eV]\,(\sigma_x^2\,[\mu m] + \frac{w_0^2[\mu m]}{4})} \approx 1.4 \times 10^6 photons/shot \tag{1}$$

with $U_L \approx 2J$, $Q \approx 200pC$, $\delta_\varphi = 0.2$, $h\nu = 1.55eV$, $\sigma_{x,y} \approx 110\mu m$ and $w_o \approx 150\mu m$ while our measured photon flux is $N_\gamma \approx 10^4 photons/pulse$.

Another contribution to the reduction of the obtained photon flux can also come from the jitter sensitivity of our $30MeV$ working point, deeply off crest in the S-band accelerating sections, as coming out from the simulation results shown in Fig. 6, where the Thomson radiation spectrum is shown as calculated with CAIN code starting from the measured parameters for the electron and photon beams (Fig.6 above) and its sensitivity to the jitter of electron beam horizontal centroid is shown in terms of photon flux reduction (Fig.6 below).

7 Conclusions

The second commissioning phase of the SPARC_LAB Thomson source took place in the June 2015 dedicated shift. The 30 MeV electron beam energy WP has been addressed as foreseen for the first planned imaging experiment. With the available hardware (only phase shifters on the 3 TW S-band sections) the applied acceleration/deceleration scheme worked well enough to produce a low energy spread electron beam

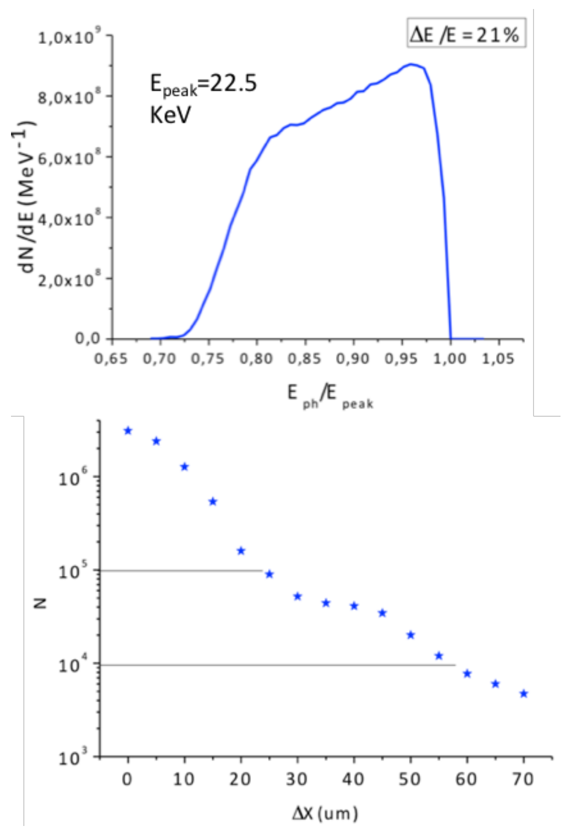

Figure 6: Thomson X-radiation spectral distribution calculated from the measured electron and laser beam parameters for this second commissioning shift (above), the relative photon flux reduction estimation coming from the jitter in the transverse electron beam centroid.

at 30 MeV, even though resulting in a strong sensitivity for the electron beam to the machine imperfections/stability. The optimization plan foresees a better control of the electron trajectory at the IP to avoid unrecoverable off-axis emission of the Thomson radiation and too high background contribution to the X-ray detectors signal. An interaction setup upgrade is also under study, coming to an non-zero angle collision in order to make it easier the electron and laser pulse trajectory control removing the on axis counter propagation that limit the room availability for both beams diagnostic.

8 List of Conference Talks by LNF Authors in Year 2015

C. Vaccarezza, The SPARC_LAB Thomson Source (EAAC15), Elba, Italy

9 Publications in Year 2015

C. Vaccarezza *et al*, Nucl. Instr. Meth. A , to be printed (NIMA 58557).

References

1. Alberto Bacci et al. *Nuclear Instr. and Meth. in Phys. Res. B*, 608:90–93, 2009.
2. Massimo Ferrario et al. *IPAC 10 Kyoto, Japan*, 2010.
3. Massimo Ferrario et al. *Nuclear Instr. and Meth. in Phys. Res. B*, 309:183–188, 2013.
4. K. Flottmann. http://www.desy.de/ mpyflo/.
5. Bruno Golosio et al. *Applied Physics Letters*, 100(164104), 2012.
6. Luca Labate et al. *Radiation Effects and Defects in Solids*, 165, 2010.
7. Piernicola Oliva et al. *Nuclear Instr. and Meth. in Phys. Res. A*, 615:93–99, 2010.
8. Cristina Vaccarezza et al. *IPAC 14 Dresden, Germany*, pages 267–269, 2014.